ELSEVIER

Journal of Structural Geology 29 (2007) 614–628

JOURNAL OF STRUCTURAL GEOLOGY

www.elsevier.com/locate/jsg

Nucleation, development and petrophysical properties of faults in carbonate grainstones: Evidence from the San Vito Lo Capo peninsula (Sicily, Italy)

Emanuele Tondi*

Department of Earth Sciences, University of Camerino, Via Gentile III da Varano, 62032 Camerino (MC), Italy

Received 30 May 2006; received in revised form 7 November 2006; accepted 17 November 2006
Available online 26 January 2007

Abstract

Detailed field mapping and microstructural and textural analyses carried out in Lower Pleistocene grainstones in the San Vito Lo Capo peninsula (in north-western Sicily) revealed document failure modes and fault development in porous carbonate grainstones. Individual compactive shear bands represent the simplest fundamental shear structures, while pressure solution processes commonly localize within previously developed compactive shear bands. In the Lower-Pleistocene carbonate grainstones of San Vito Lo Capo peninsula, composed of eroded carbonate and marl fragments, pressure solution processes localize mostly grain-to-grain, leading to the formation of zones of weakness which facilitate slip and significant displacement. The transition from one deformation process to another is likely controlled by changing material properties and anisotropy within the bands. Finally, laboratory analyses of representative fault rock samples show that the structures described above have sealing capacity with respect to the host rock, and may compartmentalize any geofluid reservoir.

Keywords: Failure modes; Compactive shear bands; Stylolites; Slip surfaces

1. Introduction

Recently, Tondi et al. (2006a) discussed a new faulting mechanism in porous carbonate grainstones, composed mostly of subangular rudist fragments, from central Italy. These authors distinguished three main deformation mechanisms: (i) deformation bands developed by compaction and shear strain localization (Antonellini et al., 1994; Shipton and Cowie, 2001; Aydin et al., 2006), (ii) stylolites formed by pressure solution (Rutter, 1983; Groshong, 1988), and (iii) subsequent shearing of stylolites (Alvarez et al., 1978; Engelder and Marshak, 1985; Peacock and Sanderson, 1995; Willemse et al., 1997; Salvini et al., 1999; Graham et al., 2003). Increased slip along band-parallel sheared stylolites, together with shearing of oblique sets of stylolites, appear to be the controlling factors in the development of a fine-grained zone of cataclasis accommodating slip in the range of 5 to 75 cm.

In this paper we analyse fault development in a different type of porous carbonate grainstones, composed of eroded carbonate and marl fragments, cropping out in the San Vito Lo Capo peninsula in north-western Sicily. Here, detailed field mapping at various scales and thin section observations allowed us to document the occurrence of several sets of deformation bands, and of pressure solution processes that took place within previously formed deformation bands. We show that pressure solution processes result in the formation, within the bands, of narrow zones of reduced grain size including residual material, which enhance shear and accommodate large displacement. Mercury-injection analysis, performed on representative specimens of deformation bands, allowed us to compute pore size distribution, assess capillary pressure, and to estimate sealing capacity for both oil and gas.

* Tel.: +39 320 438 1432; fax: +39 073 740 2644.
E-mail address: emanuele.tondi@unicam.it

0191-8141/$ - see front matter © 2006 Elsevier Ltd. All rights reserved.
doi:10.1016/j.jsg.2006.11.006

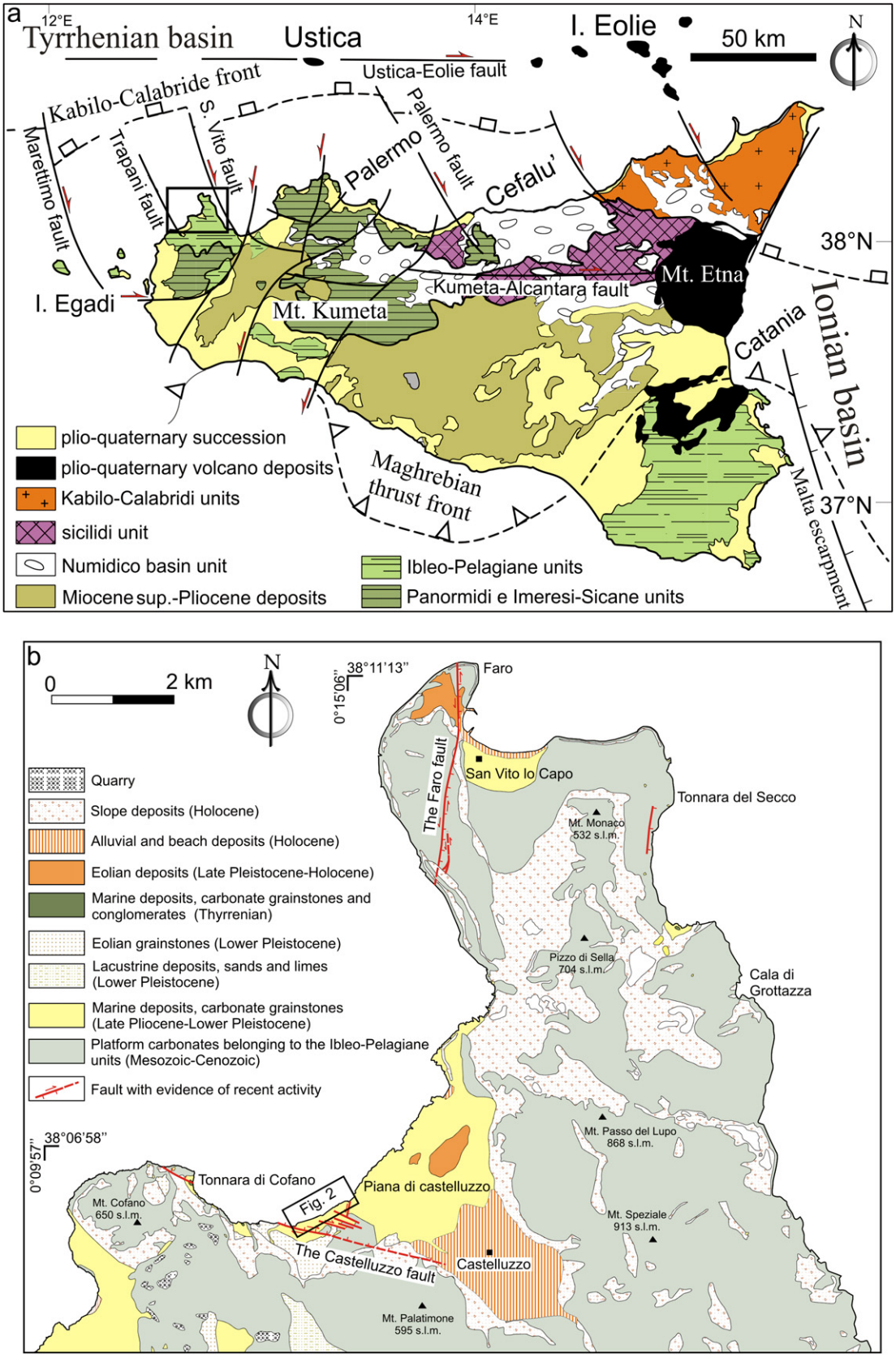

Fig. 1. (a) Schematic geo-structural map of Sicily (after Giunta et al., 2004) (b) Geological map of Plio-Pleistocene deposits cropping out in the San Vito lo Capo peninsula. Maps are slightly modified from Tondi et al. (2006b).

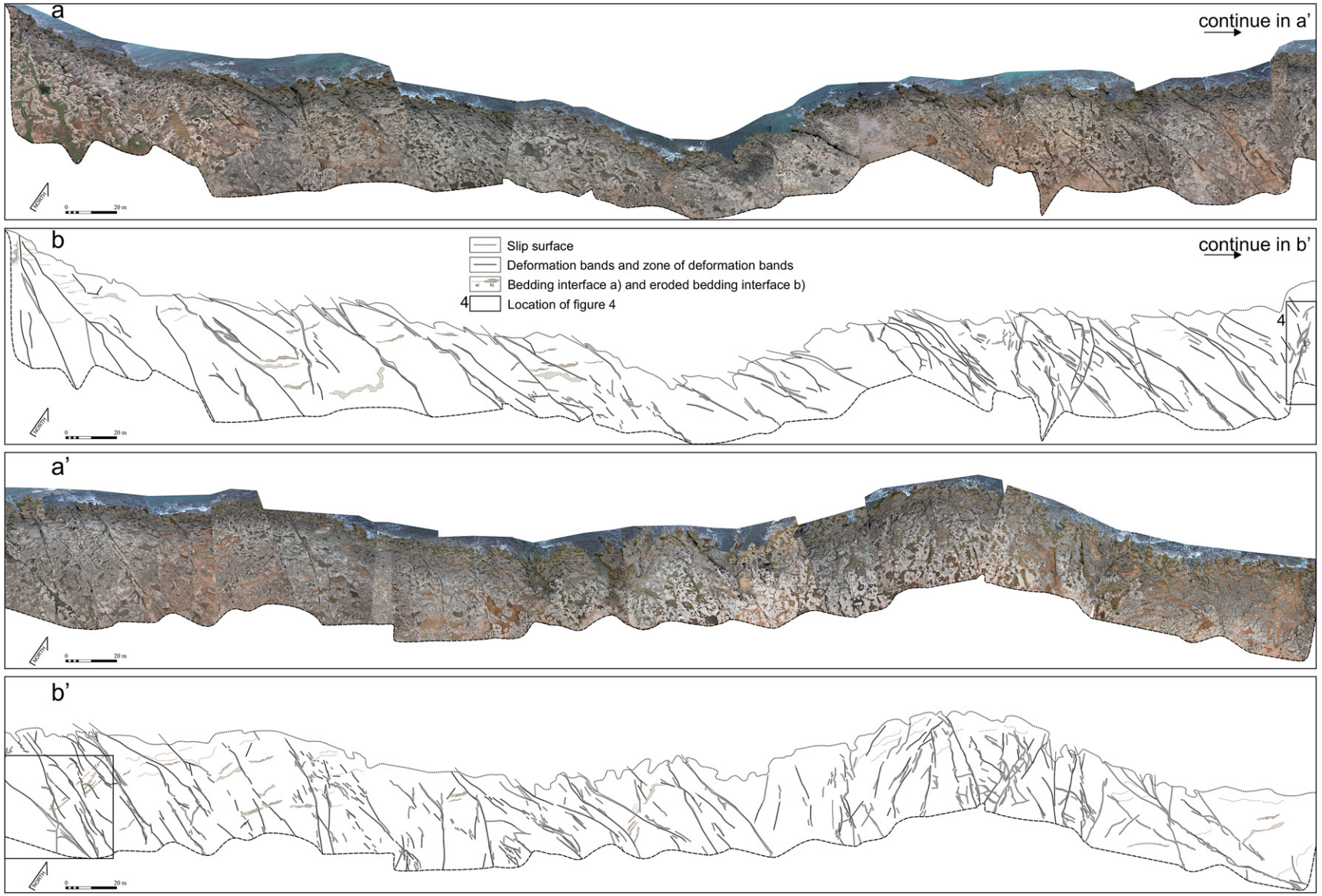

Fig. 2. Structural map of the outcrop located along the coast of Piana di Castelluzzo. The analyzed images were digitally acquired from a helicopter flying at about 50 m altitude. (a) Plan view photograph and (b) map; (a′) and (b′) represent the continuation in ENE directions of (a) and (b).

We relate observed variations in the deformation processes to: (i) the evolving mechanical behaviour of the deforming rocks, (ii) the composition of the grainstones, and (iii) to the local structural framework imposed by the currently active stress field operating in north-western Sicily (Tondi et al., 2006b).

2. Geological framework

The San Vito lo Capo peninsula, located in NW Sicily, extends in northerly direction into the southern Tyrrhenian Sea (Fig. 1a). This area represents the westernmost and the most external sector of the Sicilian orogenic belt, which is composed mainly of south-verging Neogene folds and thrusts (Fig. 1a; Ogniben, 1960; Scandone et al., 1974; Catalano et al., 1979; Catalano and D'Argenio, 1982; Giunta et al., 2000). According to some authors (i.e. Nigro et al., 2000; Renda et al., 2000; Gueguen et al., 2002; Giunta et al., 2004; Tondi et al., 2006b), the most recent faults mapped in north-western Sicily are part of a grid of high-angle faults including right-lateral roughly E–W striking structures and left-lateral meanly N–S trending features. This fault grid is related to a regional right-lateral shear zone bounded to the north by the Ustica–Eolie fault, and to the south by the Kumeta–Alcantara fault (Boccaletti et al., 1982; Ghisetti and Vezzani, 1984; Finetti and Del Ben, 1986). This shear zone accommodates the regional strain induced by the current stress field acting in the area which, as revealed by both structural and seismological data, is characterized by a NW–SE striking main compression.

Related to the above faults, some minor shear zones are well exposed in north-western Sicily (Giunta et al., 2004). Based on geometric and kinematic characteristics, these have been grouped into three major sets: (i) an ESE striking mainly right-lateral to transtensive set, (ii) a N–S striking left-lateral to transtensive set, and (iii) a NE–SW striking set including faults with left-lateral transpressive and reverse kinematics. Some of these high-angle faults involve Pliocene and Lower Pleistocene deposits. At San Vito lo Capo peninsula (Fig. 1b) in particular, two fault zones (trending roughly ESE and NNE) cut through both conglomerates of Tyrrhenian age and Holocene sediments. In this area, deformed Mesozoic to Cenozoic platform carbonates evolving upwards into deep-water marls, limestones and siliciclastic deposits are representative of the basement units underlying the marine deposits of Plio-Pleistocene age largely cropping out in the coastal plain of Castelluzzo (Piana di Castelluzzo; Fig. 1b; Abate et al., 1993, 1998). The latter deposits are well exposed and consist of carbonate grainstones, composed of eroded carbonate and marl fragments with bedding surfaces represented by unconformities between grainstone layers. These surfaces, generally not easily recognizable in outcrop, define a tabular structure with a spacing of 20 cm to 50 cm. The general dip is towards the NW, and the mean orientation is 320°/05°. Along the coast, some small outcrops of Tyrrhenian conglomerates also exist (Fig. 2).

3. Field observations

At San Vito lo Capo, the two main active faults shown in the map of Fig. 1b (Tondi et al., 2006b) are oriented roughly NNE (the Faro fault) and ESE (the Castelluzzo fault). The Faro fault shows a left-lateral component of motion and is well exposed over a length of about 3 km, whereas the Castelluzzo fault is a right-lateral strike-slip feature which is exposed for about 2 km within the Lower Pleistocene marine sediments of the San Vito Lo Capo peninsula (Fig. 1b). In the Piana di Castelluzzo, the Lower Pleistocene carbonate grainstones are also cut by several lower-rank faults (Fig. 1b). In this location, we constructed a detailed map (1:25 scale) combining field data and image analysis of a mosaic of digital photos taken from a helicopter (Fig. 2). In addition, detailed maps at 1:1 scale were constructed using string lines and detailed rectangular grid methods.

The results of our field mapping allowed us to recognize a major set of deformation bands trending ESE and two subordinate sets trending roughly NW and N (Figs. 2 and 3). The geometry of the step-over zones and the offset of bedding and older structures across them indicate a right-lateral strike-slip character for the ESE striking set and a left-lateral strike-slip kinematics and oblique-normal for (subordinate) ones trending roughly N and NW respectively (Figs. 2 and 4). The above sets of deformation bands have an almost vertical dip and show cross-cutting relationships which suggest that they developed contemporaneously (Fig. 2). They include either individual bands, or zones of several individual bands (Fig. 5a and b). Individual deformation bands are between 1 mm and 2 mm thick, whereas the zones of deformation

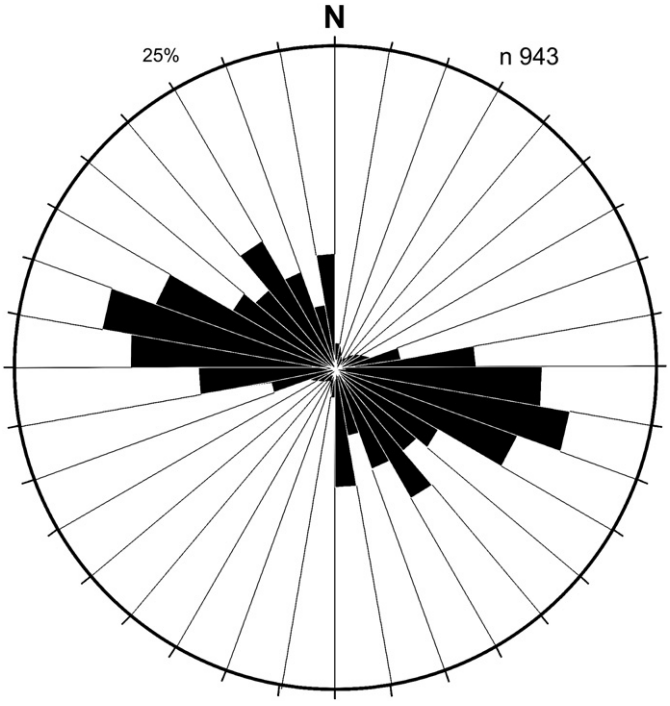

Fig. 3. Rose diagram of deformation bands and slip surfaces measured on the Piana di Castelluzzo.

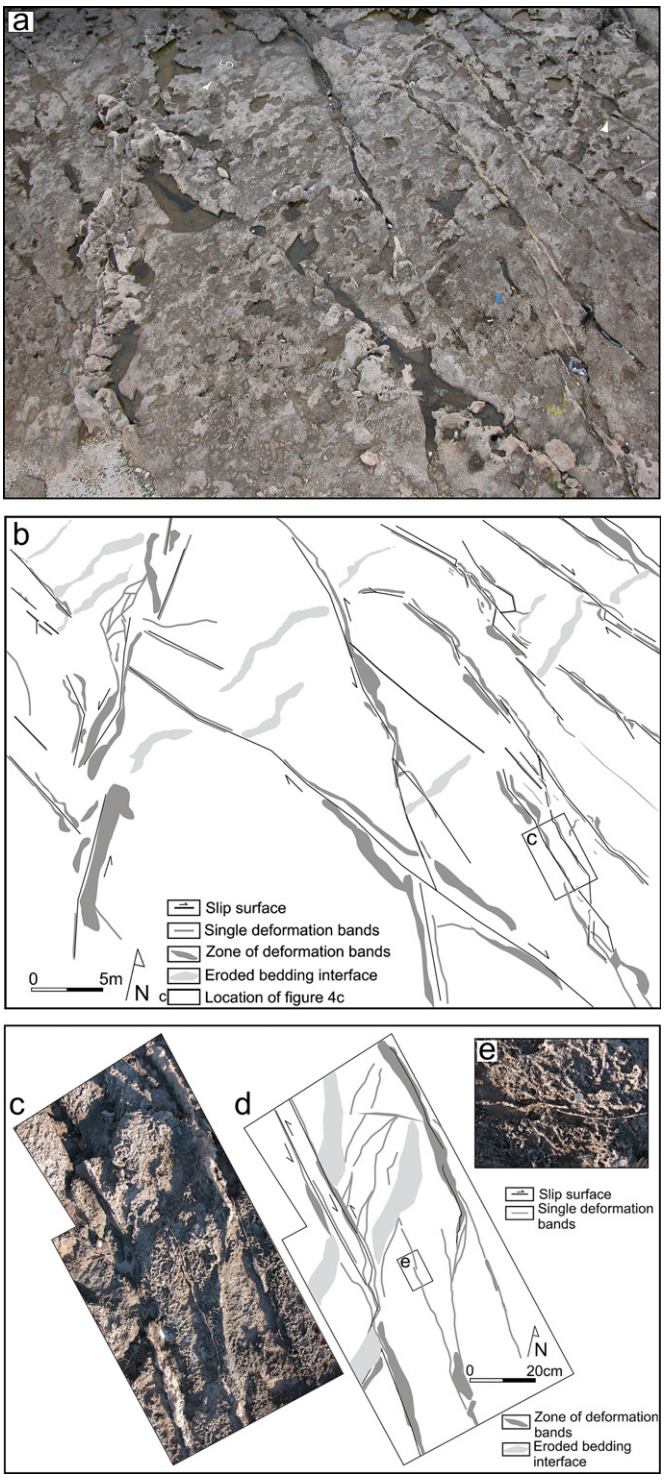

Fig. 4. ESE, NNW and N striking deformation bands, (a) photograph and (b) map (see Fig. 2b for location). The bands generally display a Riedel-like pattern and mutually cross-cutting relationships show that they formed contemporaneously. In (c) (photograph) and (d) (map) bedding interfaces are offset in left-lateral sense of about 20 cm across NNW striking deformation bands (see (b) for location). (e) shows an overlapping zone between two single deformation bands (see (d) for location).

bands range from 2 mm to 20 cm in thickness. The strike-slip zones of deformation bands are straight and narrow (Figs. 2 and 4) and occasionally display a Riedel-like pattern (Ahlgren, 2001; Katz et al., 2004). The zones of deformation bands with a normal sense of slip have a typical anastomosing pattern with interlinked eye and ramp structures (Fig. 2) (Antonellini and Aydin, 1995).These features are reminiscent of those deformation bands occurring in the porous carbonate grainstones of the Majella Mountain (Tondi et al., 2006a) and consist of light-coloured bands with respect to the parent rock; these features are easily recognized due to their increased resistance to weathering with respect to the host-rock (Figs. 2 and 4).

A narrow, red coloured zone is generally associated with all three sets of deformation bands (Fig. 5c). In outcrop, these zones commonly show a negative relief (Fig. 5d) and consist of a zone of reduced grain size including residual material and striated slip surfaces across which bedding and older structures are offset (Fig. 5e and f). Due to a lack of evident markers, we were not able to estimate the maximum offset associated with the main fault zones. This estimate was possible only for small offsets where markers are clearly recognizable (i.e. in Fig. 4c and d).

Where small outcrops of Tyrrhenian conglomerates occur along the coast of the Piana di Castelluzzo, these younger sediments commonly fill the negative relief associated to the deformation bands. Furthermore, they are also affected by the deformation (Fig. 6a and b) together with the Dendropoma coastal reef platform, which consists of worm populations that are still growing nowadays in the temperate climate of northwestern Sicily (Fig. 6c and d; Antonioli et al., 1999).

4. Petrophysical properties

The representative structural elements exposed in the Piana di Castelluzzo were sampled and examined in the laboratory by optical and scanning electron microscopy (SEM). We sampled individual deformation bands, zones of deformation bands with a narrow zone of reduced grain size, residual material and slip surfaces, as well as zones of deformation bands infilled with Tyrrhenian sediments. In addition, mercury-injection analysis was performed on representative specimens of deformation bands in order to estimate pore size distribution, capillary pressure and their sealing potential for both oil and gas.

4.1. Microstructural and textural characterization of deformation bands

We examined several samples of deformation bands and the associated structures, measuring porosity and grains-to-matrix percentage within the bands and in the surrounding host rock (samples 1 to 20 in the first row in Table 1). After the construction of accurate maps from thin section photographs, measurements were made using an automatic pixel counting with a resolution of less than 1%.

The host rock is a poor-to-medium consolidated grainstone. Grains are made up of fragments of carbonates, marls and

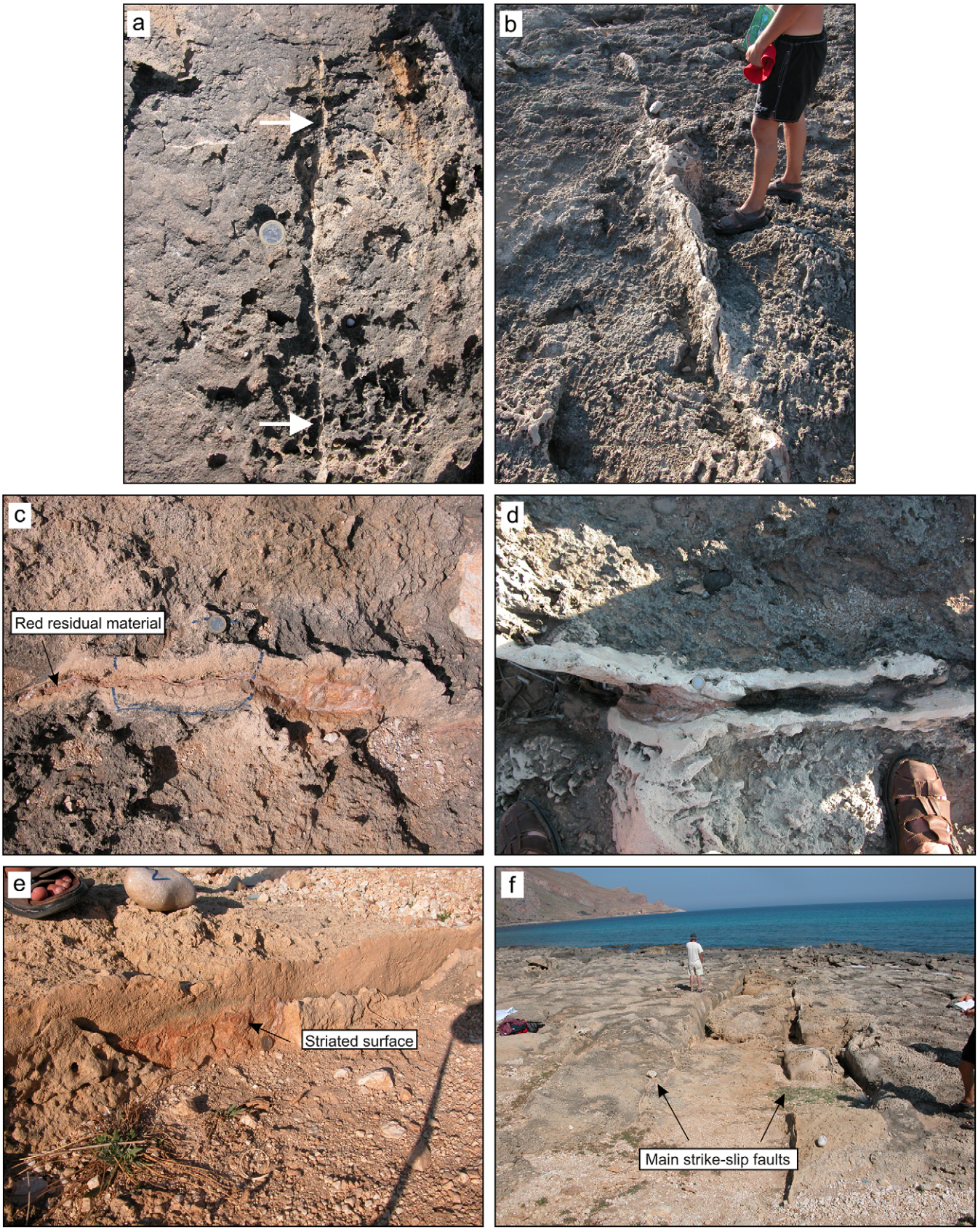

Fig. 5. Structures cropping out in the Piana di Castelluzzo. (a) Individual deformation band; (b) zone of deformation bands—note the positive relief due to their increased resistance to weathering with respect to the host-rock; (c) deformation bands with a narrow, red coloured zone of reduced grain size and residual material commonly showing a negative relief (d), due to erosion along the weaker residue material marking the structure. (e) Band-parallel slip surfaces indicated by a striated surface; (f) the main E−W-striking right-lateral fault zone. The zone includes deformation bands, a zone of reduced grain size and residual material and slip surfaces.

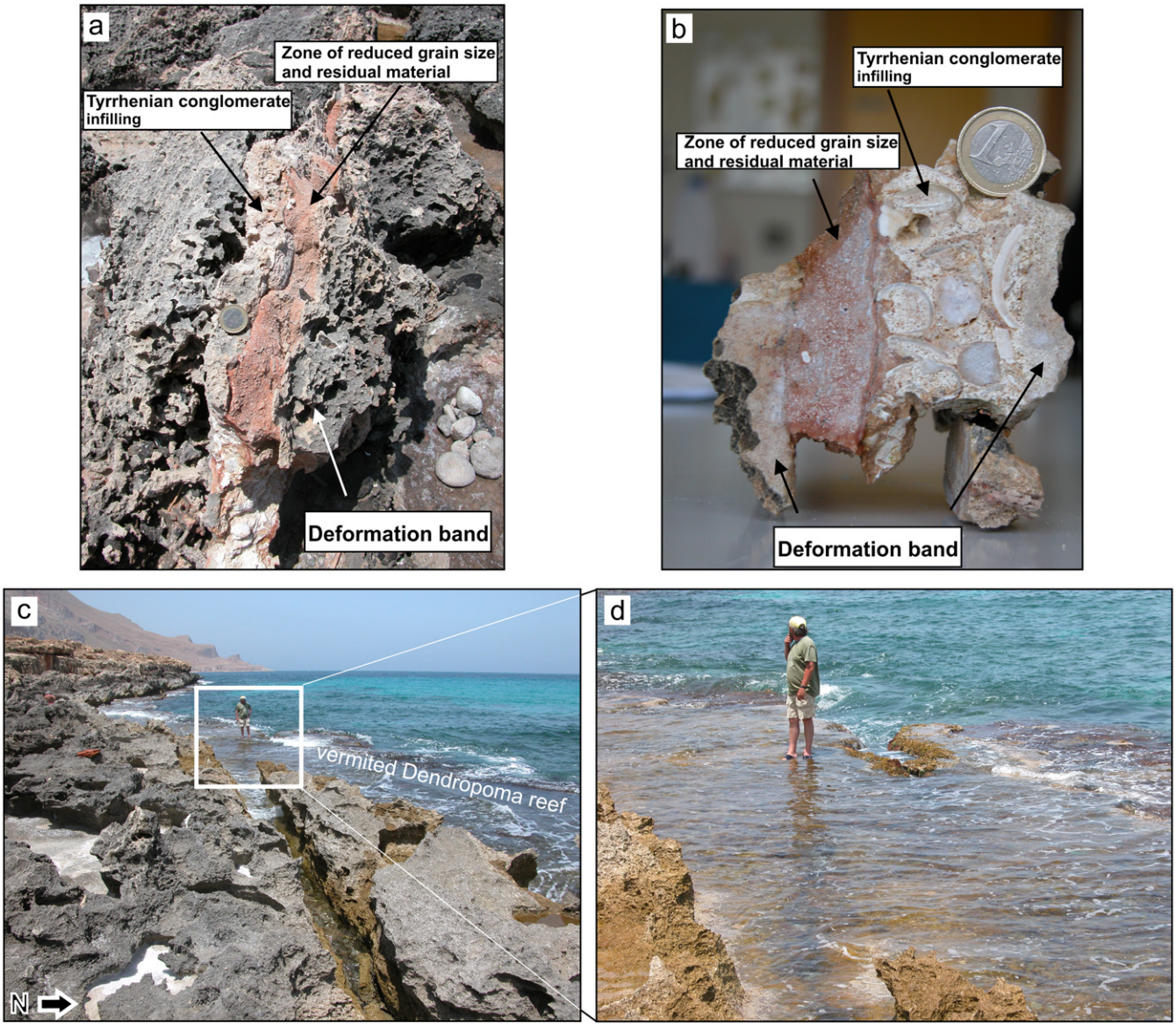

Fig. 6. Evidence of recent activity of the analysed structures (see also Tondi et al., 2006b). Deformation bands are infilled with Tyrrhenian conglomerate as shown (a) in plan and (b) in section view; (c) and (d) fault-controlled morphology of the Dendropoma reef platform.

shales ranging from 0.05 to 1 mm in diameter (Fig. 7a and b). Grains make up about 53% of the rock volume. The matrix consists of bladed and sparry calcite cement and carbonate and marl fragments smaller than 0.05 mm; these make up about 22% of the rock volume (Table 1). The average porosity is about 24%. The values of the grains-to-matrix ratio in the host rock fall between 2.0 and 3.0, with porosities between 19% and 30%.

In thin section deformation bands show a different texture from the parent rock (Fig. 8a and b). The inner parts of the

Table 1
Grains, matrix and porosity percentage in the host rock and in Zones I, II and III of the deformation bands

	Host rock				Zone III				Zone II					Zone I						
Sample	1	2	3	4	5	6	7	8	9	10	11	12	13	14	15	16	17	18	19	20
Grain %	54.5	52.8	50.8	54.4	56.6	58.5	56.7	57.1	54.2	54.3	76.7	70.2	71.4	69	71.8	9.4	6.1	5.6	5.7	10
Matrix %	26.7	22	19.2	24.9	18.6	37	37.9	40	39.9	38.9	20.9	28.9	24.5	29.1	25.3	90.6	93.9	94.4	94.3	90
Porosity %	18.8	25.2	30	20.7	24.8	4.5	5.4	2.9	5.9	6.8	2.4	0.9	4.1	1.9	2.9	0	0	0	0	0
Grain to matrix ratio	2.0	2.4	2.6	2.2	3.0	1.6	1.5	1.4	1.4	1.4	3.7	2.4	2.9	2.4	2.8	0.1	0.1	0.1	0.1	0.1

The ratio between grain and matrix is also shown. Mean error is on the order of 1%.

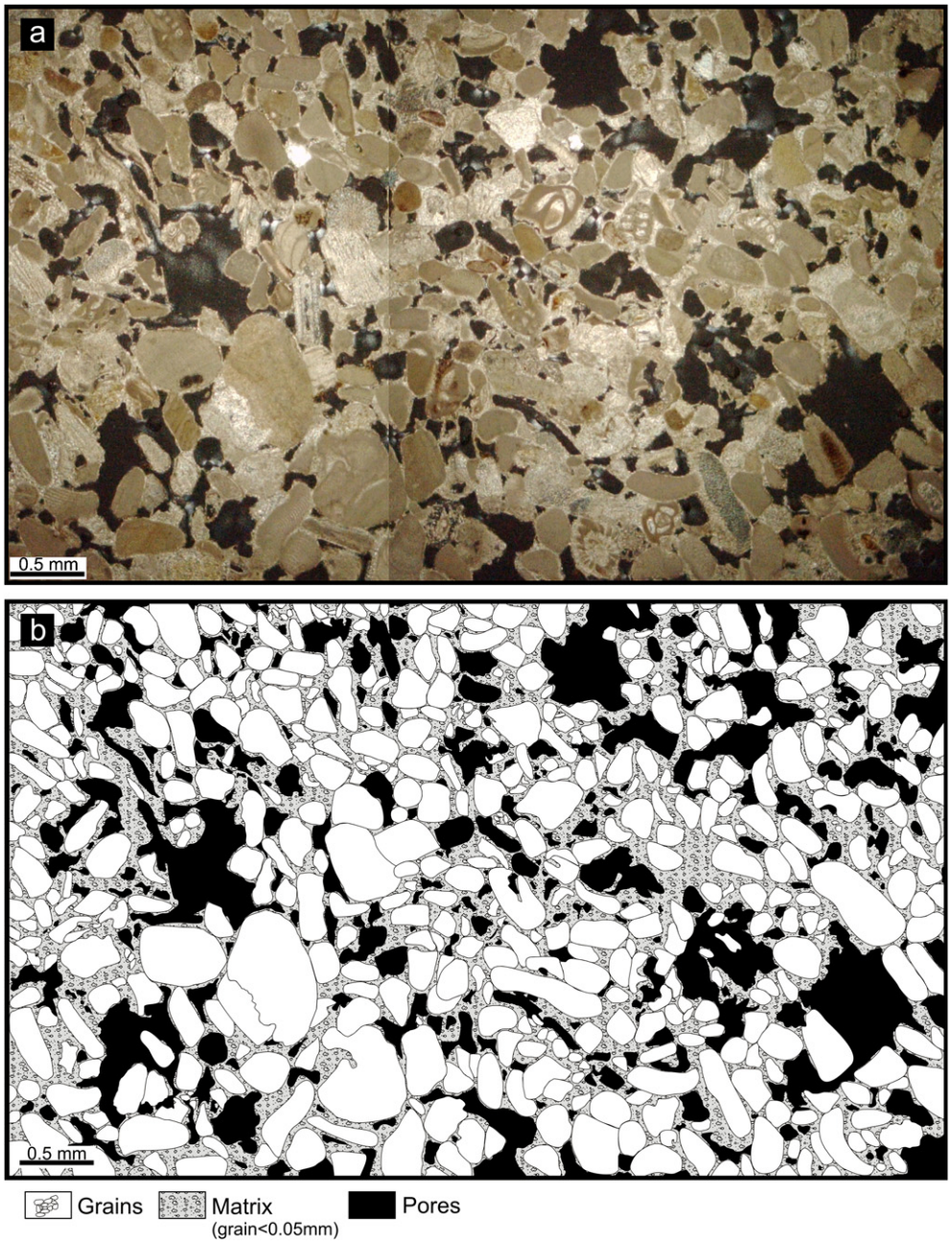

Fig. 7. (a) Photograph and (b) map of the host rock, which is composed of eroded carbonate and marls fragments and matrix. Porosity ranges between 19% and 30%.

bands are characterized by a well-developed, continuous zone of grain size and porosity reduction (Zone I in Fig. 8a and b). These zones are bounded on both sides by a compacted grain zone, usually measuring one-half the inner parts of the band thickness, where the ratio of grains to matrix is constant at between 2.4 and 3.7 (mean value 2.8) of that in the host-rock (bottom row of Table 1) indicating no grain size reduction (Zone II in Fig. 8a and b). Zone I, represented by a reduced grain size, and Zone II, represented by compacted grains, are bounded on both sides by a wide area (Zone III in Fig. 8a and b) where the grains-to-matrix ratio is 1.35–1.58 and porosity is 3–6%. This Zone has a texture strikingly different from Zones I and II. In fact, if porosity is reduced, grains occupy the same percentage (about 56% of the rock volume) of the host rock indicating no compaction. In the Zone III of the band, the matrix, mostly consisting of calcite cement (Fig. 9a and b), makes up about 39% of the rock (Table 1).

Deformation bands are in most cases overprinted by stylolites (Figs. 8a,b and 9c). These are mostly localized grain-to-grain and are marked by a ~0.001 to 0.01 mm thick red film showing columnar and wavy forms with average amplitude of 0.01 mm. Several stylolites are recognizable in Zone II (see Fig. 8a and b).

In an individual deformation band, we were able to observe the incipient formation of the three Zones described

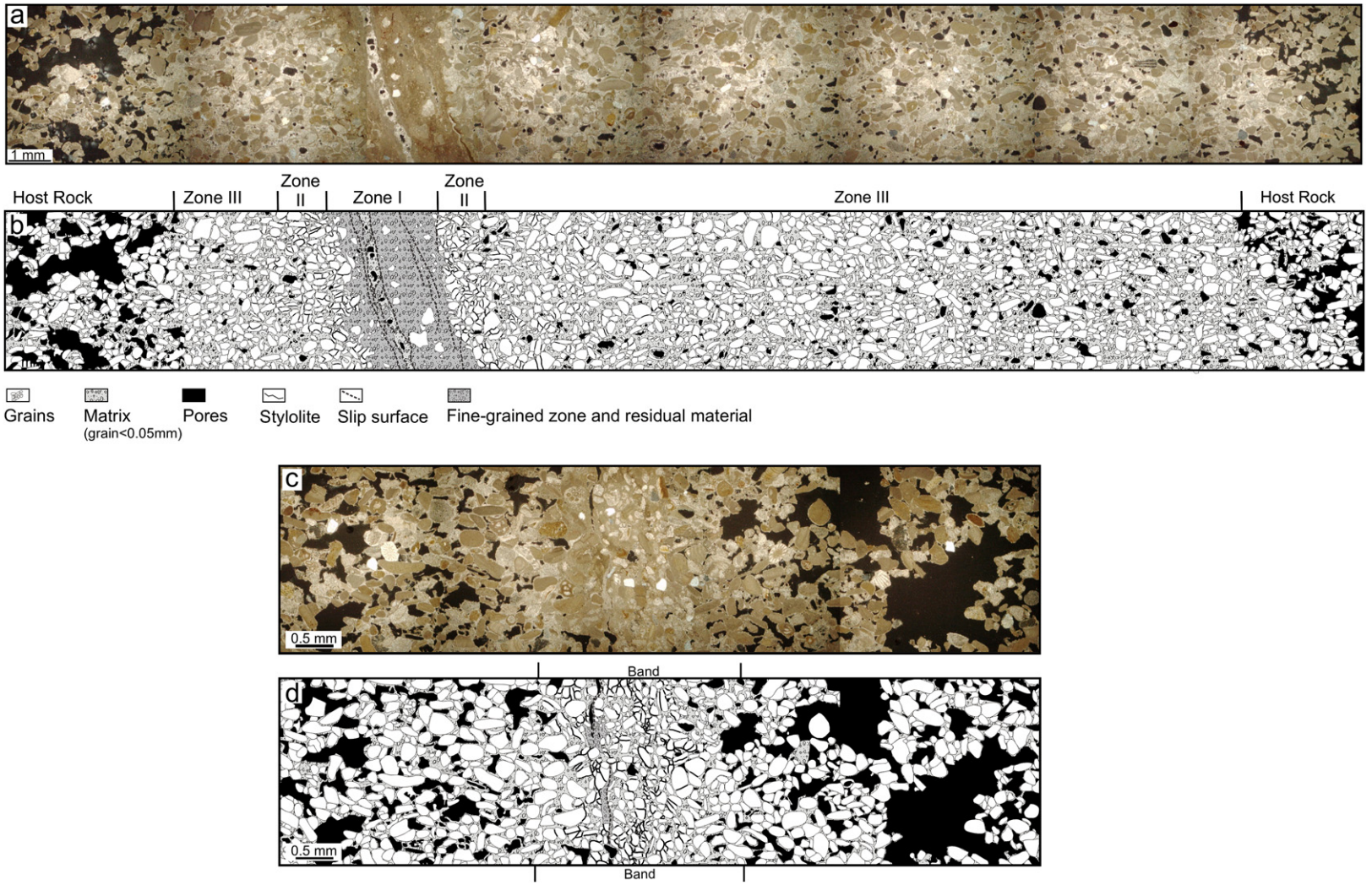

Fig. 8. Deformation band characterized by tabular zones (Zones I, II and III) with different texture (see text for descriptions); (a) photographs and (b) map. Individual deformation band with incipient Zones formations are illustrated in (c) a photograph and (d) a map. Associated with the slip surfaces (Zone I) are open pores, in some case partially infilled with calcite cement (Fig. 8a).

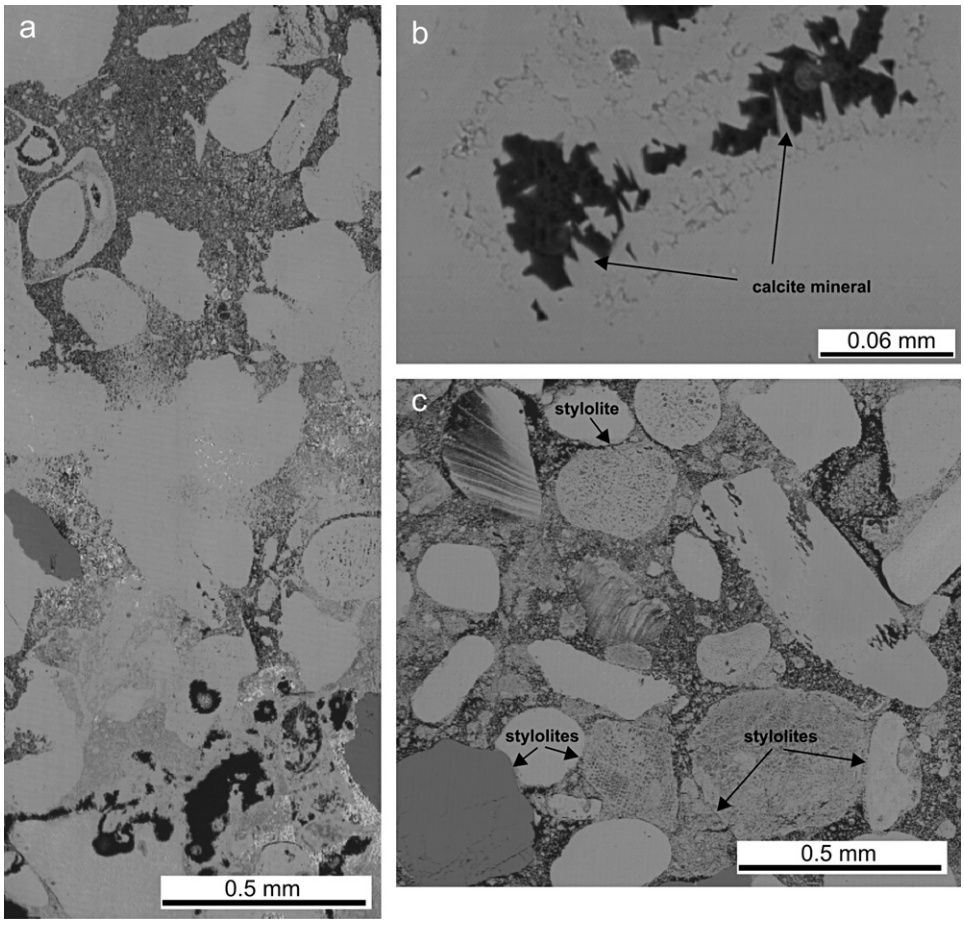

Fig. 9. (a) SEM image of Zone III of deformation bands, in which pores are infilled by calcite (b); (c) Zone II of a deformation band, here the stylolites, mostly localized grain-to-grain contacts, are easily recognizable.

above (Fig. 8c and d). The inner part of the bands shows in fact a few thin and discontinuous pockets of fine material (likely represented by residual material as suggested by its red/brown colour) within a zone where several stylolites are recognizable and where grain size are reduced with respect to the parent rock. Within the thin and discontinuous pockets of fine material it is also possible to observe some slip surfaces, as evidenced by the associated open space (Fig. 8c and d); these, however, are better developed in the more continuous and better developed Zone I of the bands (refer to Figs. 8a,b and 10). Zone I, characterized by the lowest grains-to-matrix ratio (0.06–0.11), as well as by the lowest porosity (less than 1%, Table 1) represents in fact an advanced stage of deformation and, in terms of petrophysical properties, appears to be similar to the fine-grained zone of cataclasis described in Tondi et al. (2006a). Our data on the relative percentage of pores, grains and matrix collected from samples representing progressive deformation stages are plotted on the triangular diagram in Fig. 11. These data show an evolving deformation path, from the host rock to deformation bands without ‘‘cataclasis’’ (Zone II of the bands), and finally to the deformation bands with ‘‘cataclasis’’ and slip surfaces (Zone I of the bands).

4.2. Capillary pressure, sealing potential and pore size distribution of deformation bands

Mercury-injection analysis allows calculation of the resistance of the deformation bands to invasion by non-wetting fluids such as gas and oil (Sneider et al., 1997; Agosta et al., in press). Fig. 12a shows the mercury-air capillary pressure as function of the cumulative percent intruded mercury up to a maximum applied 59,000 psia.

Capillary pressure tests were performed on six samples (from C1 to C6). Samples C1, C2, C3 are representative of Zone III of the deformation bands, whereas C4, C5, C6 contain both Zones I and II of the bands (due to their narrow width, we were not able to investigate separate samples of Zones I and II). Samples C1, C2 and C3 show a breakthrough pressure at 10% of the cumulative intruded mercury, ranging from 2.63 to 3.20 psia (with a mean value of 2.80 psia); whereas C4, C5, C6 samples show values ranging from 6 to 17 (with a mean value of 12 psia (Fig. 12a).

Based on these mean values, we evaluated the sealing potential of Zone III and of Zones II and Zone I of the bands using representative fluid properties for both oil and gas and the following equations (Sneider et al., 1997):

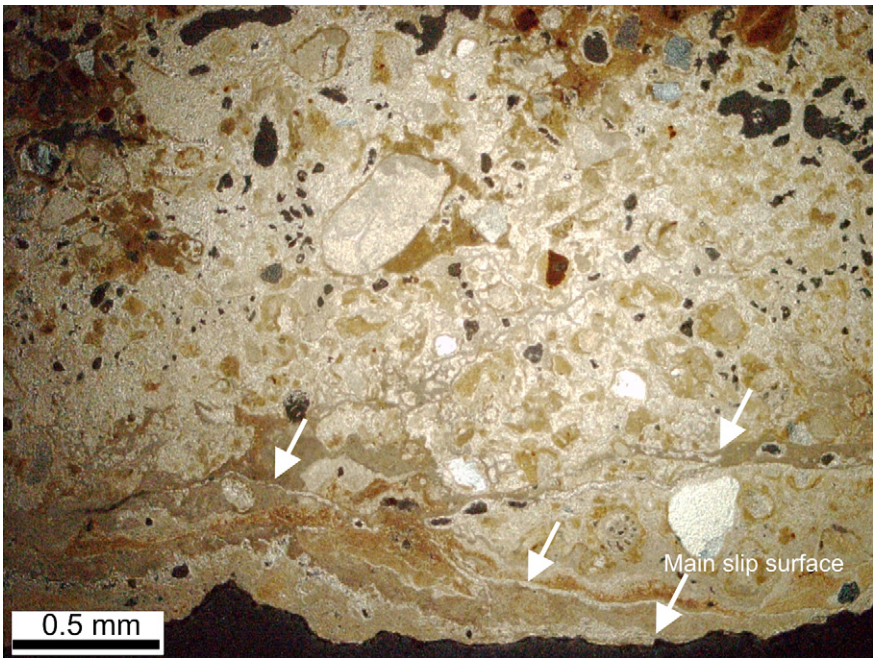

Fig. 10. The inner part of the deformation bands (Zone I) characterized by a well-developed and continuous slip surfaces (white arrows), is oriented nearly parallel to the band boundaries. Slip surfaces, characterised by striated surfaces in the field, are marked by a ~0.001 to 0.005 mm thick layer of red, brown or grey material with an average width of 0.005 mm.

$$\mathrm{Pc}_{h/w} = \left[\left(\sigma_{h/w}\cos\theta_{h/w}\right)/\left(\sigma_{\mathrm{Hg/air}}\cos\theta_{\mathrm{Hg/air}}\right)\right]\mathrm{Pc}_{\mathrm{Hg/air}} \quad (1)$$

and

$$H = \mathrm{Pc}_{h/w}/\Delta\rho\ 0.4333 \quad (2)$$

Where Pc is the capillary breakthrough pressure, H is the maximum hydrocarbon height, σ is the interfacial tension between hydrocarbon and brine, θ is the contact angle, and $\Delta\rho$ is the difference in tension between hydrocarbon and brine. Subscripts h, w, and Hg refer respectively to hydrocarbon, water and mercury. Input parameters used to compute the maximum sealable hydrocarbon column height are those provided by Sneider et al. (1997).

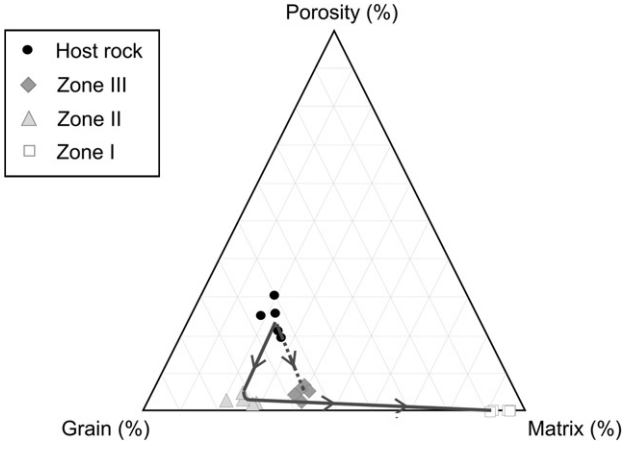

Fig. 11. Percentage of pores, grains and matrix of deformation bands. Continuous line with arrows indicates the deformation path from the host rock to deformation bands without "cataclasis" (Zone II of the bands), and finally to the deformation bands with "cataclasis" and slip surfaces (Zone I of the bands). Dotted line depicts the evolution from host-rock to Zone III of the band.

Zone III of the deformation bands shows a sealing potential which is about 5 m for gas and 10 m for oil. Zones II and I of the bands show a major sealing potential which is about 15 m for gas and 35 m for oil. According to the Sneider Seal Classification (Sneider et al., 1997), Zone III falls in the category of a class E seal (<15 m oil), whereas Zones II and I fall in the category of class C seal (30–150 m oil). Furthermore, because the relative volume of intruded mercury (incremental intrusion in Fig. 12b) yields information on the relative proportions of individual pore sizes (pore diameter in Fig. 12 b), we used the results of capillary pressure analysis to compute the pore size distribution for representative samples (from C1 to C6) of deformation bands. In Fig. 12b it is emphasised that the relative shape of the curves as well as the more representative diameter values (given by the mean peaks), clearly depict two groups: (i) a group represented by samples C1, C2 and C3, which are representative of Zone III of the deformation bands, and (ii) a group represented by samples C4, C5 and C6, representative for Zones II and I of the bands. It is clear that the pore-size distribution of each group is almost identical and that the main peaks for the first group (C1, C2, C3) correspond to pore radii of about 100 μm, whereas the main peaks for the second group (C4, C5 and C6) correspond to pore radii of 10 to 0.1 μm.

5. Discussion

The porous carbonate grainstones cropping out along the coast of the Piana di Castelluzzo are pervasively affected by individual deformation bands and zones of deformation bands with slip surfaces. All sets of deformation bands show both

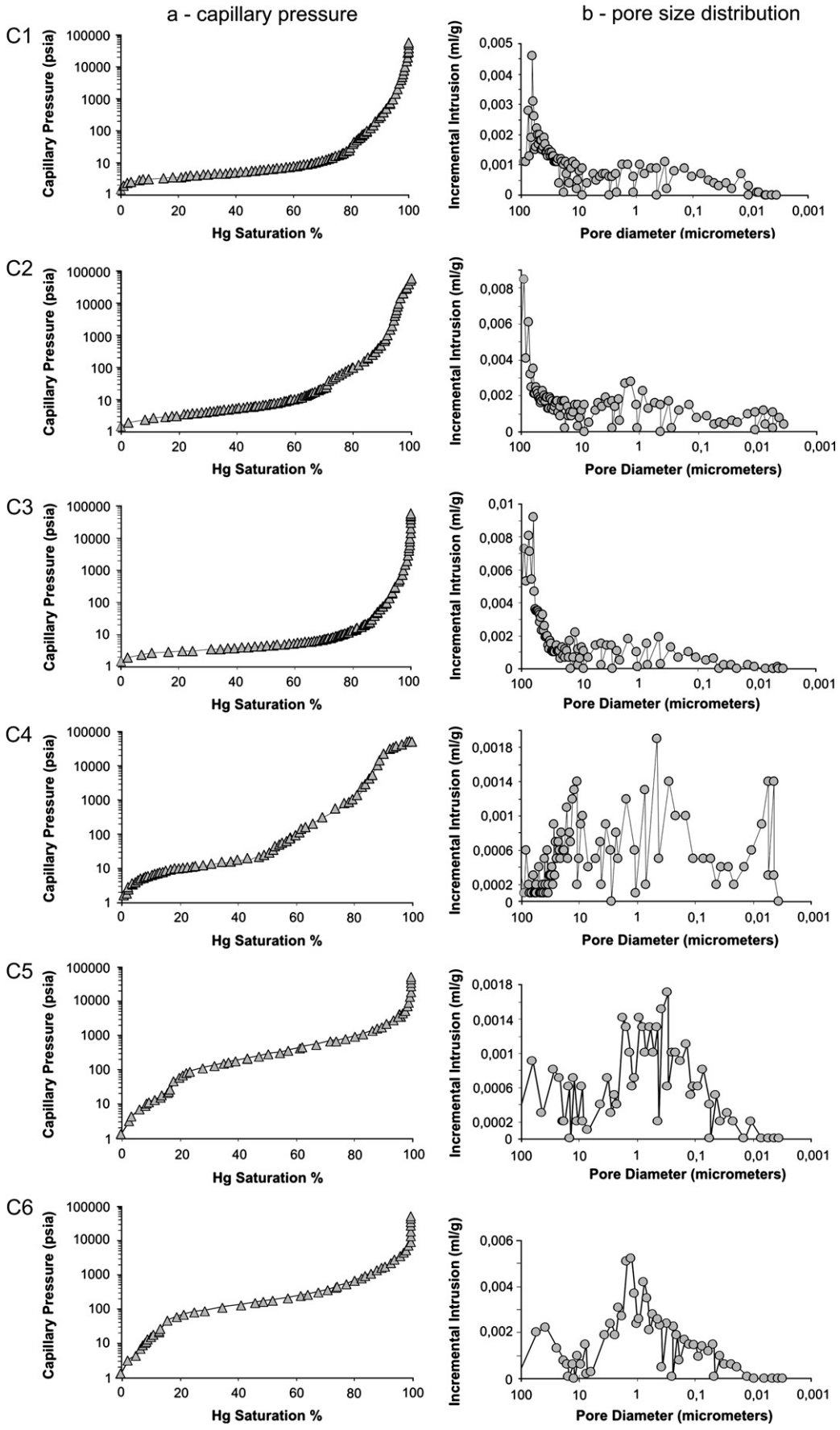

Fig. 12. (a) Capillary pressure and (b) pore size distribution of deformation bands. C1, C2, C3 are samples representative of Zone III of the deformation bands, whereas C4, C5, C6 are samples representative of both Zone II and I of the bands.

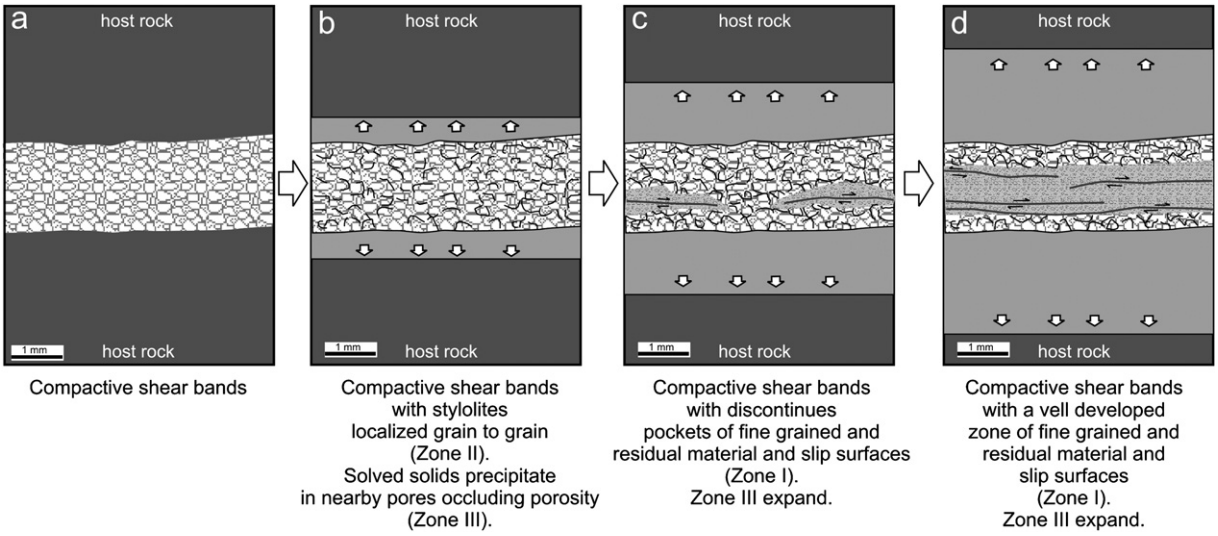

Fig. 13. Evolution of faults within the compactive shear bands in the Lower-Pleistocene grainstones cropping out along the Piana di Castelluzzo.

porosity reduction and shearing and are, therefore, classified as compactive shear bands (Bésuelle, 2001; Aydin et al., 2006). Among these, individual compactive shear bands with no slip surfaces, grain breakage, and/or ''cataclasis'' represent the simplest fundamental shear structures formed in this type of porous carbonate grainstone (Fig. 13a).

The mechanism of compactive shear bands documented in this paper is similar to what it has been described by Tondi et al. (2006a), which involves grain translation and rotation with pore collapse. This mechanism, observed in several limestone samples deformed in the laboratory (Baud et al., 2000; Vajdova et al., 2004), results in a tight band with a noticeable shear displacement gradient. The presence of the tight bands is consistent with an estimated high initial porosity (15–30%) of the Lower-Pleistocene carbonate grainstones, and with its thin overburden (Tondi et al., 2006b).

Within the compactive shear bands, pressure solution processes responsible for the stylolites occur at contacts between grains (Fig. 13b). Even though stylolites are produced by different processes, they are kinematically compatible. Therefore, the transition from one mode to another does not require drastic changes in loading conditions. The result is an additional intergranular compaction, which is most strikingly visible as sutured intergranular contacts (Zone II of the bands in Fig. 13c). In this Zone of the bands, intergranular pressure solution destroys all pore space with no cementation, so that the rock consists of sutured grains with no intergranular space at all, resulting in a ''fitted fabric'' texture. Increased intergranular pressure solution, determining the dissolution of part of the grains, generates grain size reduction and a large amount of residual material (Zone I of the bands in Fig. 13c). Within Zone I, similar to the cataclastic deformation zones described in earlier studies (Engelder, 1974; Aydin, 1978; Aydin and Johnson, 1978), several slip surfaces are present (refer to Figs. 5e,f and 10). Intergranular pressure solution also generates solved solids that precipitate in nearby pores occluding porosity (Zone III of the bands in Fig. 13c). The residual porosity of Zone III, which ranges between 3% and 6%, could be considered as the moldic porosity of the analysed porous grainstones.

It has been noted that cataclasis in compactive deformation bands in carbonate grainstones occurs by pressure solution and by the formation of discrete stylolites (anti-cracks; Fletcher and Pollard, 1981) which are subsequently sheared (Tondi et al., 2006a). The cited authors have also shown how increasing slip along the sheared stylolites is an efficient mode of rock fragmentation producing a fine-grained zone of cataclasis within the bands. On the contrary, in the Lower-Pleistocene carbonate grainstones of the San Vito Lo Capo peninsula, grain size reduction occurs by intergranular pressure solution and by the resulting grain dissolution. These fine-grained zones, rich in residual host-rock components that are not pressure-dissolved (usually clay minerals), represent weak zones within the bands, which facilitate slip and larger displacement.

Our observations indicate that compactive shear bands are the oldest structures formed in the Piana di Castelluzzo area since the lower Pleistocene, whereas the mesofaults affecting the Tyrrhenian sediments and the Dendropoma reef (characterized by distinctive slip surfaces, gouge, and the same kinematics as the compactive shear bands) developed later. This also suggests that the geometry of the stress field acting in the area and characterized by a maximum compression oriented roughly NW (see also Cello et al., 1997; Goes et al., 2004; Tondi et al., 2005, 2006b) has not changed since the Lower Pleistocene.

6. Conclusions

Field mapping and microstructural and textural analyses allowed documentation of failure modes and fault development in porous carbonate grainstones cropping out in the San Vito Lo Capo peninsula (north-western Sicily, Italy). The process of fault nucleation and development in porous carbonate grainstones that were covered by a thin overburden, as in the studied rocks, can be by a variety of mechanisms such as grain translation and rotation, grain fracturing, pressure solution,

and dilatant microcracking. Based on the data collected along the strike-slip faults present in the San Vito Lo Capo peninsula, the two major mechanisms responsible for their development have been identified as: (1) strain localization into narrow bands, and (2) intergranular pressure solution.

The products of the first process are three sets of compactive shear bands which are characterized by a particulate flow mechanism involving grain rotation, translation and pore collapse. The products of the pressure solution process are stylolites which occur at contacts between grains and overprint the earlier individual sets of compactive shear bands. Intergranular pressure solution also generates solved solids that precipitate in nearby pores occluding porosity.

Interactive failure processes involving strain localization into bands and pressure solution have been previously recognized in carbonates (Tondi et al., 2006a). In this paper we document an additional example of these interactive processes in which pressure solution plays a different role from that described in Tondi et al. (2006a). Here, increased intergranular pressure solution within the bands results in the dissolution of part of the grains, producing grain size reduction and a large amount of residual material. These narrow zones, which in terms of petrophysical properties are similar to cataclastic deformation zones, represent weak zones which facilitate slip and the development of larger displacement. Furthermore, laboratory analyses of representative fault rock samples show that the structures described above have sealing capacity with respect to the host rock and may compartmentalize a reservoir or aquifer in the subsurface.

Finally, we conclude that the evolving fault growth process depicted for the carbonate grainstones of the San Vito Lo Capo peninsula requires that the geometry of the stress field acting in the area did not change from Lower-Pleistocene times to the Present.

Acknowledgements

This work has been supported by University of Camerino (research funds to E.T.), by the MIUR, Cofin 2005 (research funds to G. Cello). I wish to thank Professor G. Giunta, Professor P. Renda and Dr M. Unti for help during the field work; Dr Mauro Alessandroni for his support on image analysis; and Professors G. Cello and F. Agosta for their suggestions during the writing of the manuscript. I am also grateful to Dr Quentin Fisher and the Sorby Multiphase Flow Laboratory in Leeds for mercury-injection analyses.

References

Abate, B., Di Maggio, C., Incandela, A., Renda, P., 1993. Carta Geologica dei Monti di Capo San Vito. Dipartimento di Geologia e Geodesia dell'Università di Palermo, Italy.

Abate, B., Incandela, A., Nigro, F., Renda, P., 1998. Plio-Pleistocene strike-slip tectonics in the Trapani Mts. (NW Sicily). Bollettino della Società Geologica Italiana 117, 555–567.

Agosta, F., Prasad, M., Aydin, A., in press. Physical properties of carbonate fault rocks, Fucino basin, central Italy: implications for fault seal in platform carbonates. Geofluids.

Antonioli, F., Chemello, R., Improta, S., Raggio, S., 1999. dendropoma lower intertidal reef formations and their paleoclimatological significance, NW Sicily. Marine Geology 161, 155–170.

Ahlgren, S.G., 2001. The nucleation and evolution of Riedel shear-zones as deformation bands in porous sandstone. Journal of Structural Geology 23, 1203–1214.

Alvarez, W., Engelder, T., Geiser, P.A., 1978. Classification of solution cleavage in pelagic limestones. Geology 6, 263–266.

Antonellini, M.A., Aydin, A., 1995. Effect of faulting on fluid flow in porous sandstones: geometry and spatial distribution. American Association of Petroleum Geologists Bulletin 79, 642–671.

Antonellini, M.A., Aydin, A., Pollard, D.D., 1994. Microstructure of deformation bands in porous sandstones at Arches National Park, Utah. Journal of Structural Geology 16, 941–959.

Aydin, A., 1978. Small faults formed as deformation bands in sandstone. Pure and Applied Geophysics 116, 913–930.

Aydin, A., Johnson, A.M., 1978. Development of faults as zones of deformation bands and as slip surfaces in sandstone. Pure and Applied Geophysics 116, 931–942.

Aydin, A., Borja, R.I., Eichhubl, P., 2006. Geological and mathematical framework for failure modes in granular rock. Journal of Structural Geology 28, 83–98.

Baud, P., Schubnel, A., Wong, T.F., 2000. Dilatancy, compaction, and failure mode in Solnhofen limestone. Journal of Geophysical Research-Solid Earth 105 (B8), 19289–19303.

Bésuelle, P., 2001. Compacting and dilating shear bands in porous rock: Theoretical and experimental conditions. Journal of Geophysical Research 106, 13435–13442.

Boccaletti, M., Conedera, C., Dainelli, P., Gocev, P., 1982. The recent (Miocene-Quaternary) rhegmatic system of western Mediterranean region. A new model of ensialic geodynamic evolution in a context of plastic/rigid deformation. Journal of Petroleum Geology 5, 31–49.

Catalano, R., D'Argenio, B., 1982. Schema geologico della Sicilia. In: Catalano, R., D'Argenio, B. (Eds.), Guida alla Geologia della Sicilia Occidentale, Guide Geologiche Regionali, Memorie della Società Geologica Italiana. Supplemento A, 24, pp. 9–41.

Catalano, R., D'Argenio, B., Montanari, L., Renda, P., Abate, B., Monteleone, S., Macaluso, T., Pipitone, G., Di Stefano, E., Lo Cicero, G., Di Stefano, P., Agnesi, V., 1979. Contributo alla conoscenza della struttura della Sicilia Occidentale: Il profilo Palermo-Sciacca. Bollettino della Società Geologica Italiana 19, 485–493.

Cello, G., Mazzoli, S., Tondi, E., Turco, E., 1997. Active tectonics in the Central Apennines and possible implications for seismic hazard analysis in peninsular Italy. Tectonophysics 272, 43–68.

Engelder, T., 1974. Cataclasis and the generation of fault gouge. Geological Society of America Bulletin 85, 1515–1522.

Engelder, T., Marshak, S., 1985. Disjunctive cleavage formed at shallow depth in sedimentary rocks. In: Hancock, P.L., Powell, C.M. (Eds.), Multiple Deformation in Ductile and Brittle Rocks. Pergamon, New York, pp. 327–343.

Finetti, I., Del Ben, A., 1986. Geophysical study of the Tyrrhenian opening. Boll. Geof. Teor. Appl. 28, 75–155.

Fletcher, R.C., Pollard, D.D., 1981. Anticrack model for pressure solution surfaces. Geology 9, 419–424.

Ghisetti, F., Vezzani, L., 1984. Thin-skinned deformation in Western Sicily. Bollettino della Società Geologica Italiana 103, 129–157.

Giunta, G., Nigro, F., Renda, P., Giorgianni, A., 2000. The Sicilian-Maghrebides Tyrrhenian Margin: a neotectonic evolutionary model. Bollettino della Società Geologica Italiana 119, 553–565.

Giunta, G., Luzio, D., Tondi, E., De Luca, L., Giorgianni, A., D'Anna, G., Renda, P., Cello, G., Nigro, F., Vitale, M., 2004. The Palermo (Sicily) seismic cluster of September 2002, in the seismotectonic framework of the Tyrrenian Sea-Sicily border area. Annals of Geophysics 47/6, 1755–1770.

Goes, S., Giardini, D., Jenny, S., Hollenstein, C., Kahle, H.-G., Geiger, A., 2004. A recent tectonic reorganization in the south-central Mediterranean. Earth and Planetary Science Letters 226, 335–345.

Graham, B., Antonellini, M., Aydin, A., 2003. Formation and growth of normal faults in carbonates within a compressive environment. Geology 31, 11–14.

Groshong, R.H., 1988. Low-temperature deformation mechanisms and their interpretation. Geological Society of America Bullettin 100, 1329–1360.

Gueguen, E., Tavarnelli, E., Renda, P., Tramutoli, M., 2002. The geodynamics of the southern Tyrrhenian Sea margin as revealed by integrated geological, geophysical and geodetic data. Bollettino della Società Geologica Italiana. Volume Speciale 1, 77–85.

Katz, Y., Weinberger, R., Aydin, A., 2004. Geometry and kinematic evolution of Riedel shear structures, Capitol Reef National Park, Utah. Journal of Structural Geology 26 (3), 491–501.

Nigro, F., Renda, P., Arisco, G., 2000. Tettonica recente nella Sicilia nord-occidentale e nelle Isole Egadi. Bollettino della Società Geologica Italiana 119, 307–319.

Ogniben, L., 1960. Nota illustrativa dello schema geologico della Sicilia nord-orientale. Riv. Min. Sic. 64–65, 184–212.

Peacock, D.C.P., Sanderson, D.J., 1995. Pull-aparts, shear fractures and pressure solution. Tectonophysics 241, 1–13.

Renda, P., Tavarnelli, E., Tramutoli, M., Gueguen, E., 2000. Neogene deformations of Northern Sicily, and their implications for the geodynamics of the Southern Tyrrenian Sea margin. Memorie della Società Geologica Italiana 55, 53–59.

Rutter, E.H., 1983. Pressure solution in nature, theory and experiment. Geological Society of London Journal 140, 725–740.

Salvini, F., Billi, A., Wise, D.U., 1999. Strike-slip fault-propagation cleavage in carbonate rocks: the Mattinata Fault zone, Southern Apennines, Italy. Journal of Structural Geology 21, 1731–1749.

Scandone, P., Giunta, G., Liguori, V., 1974. The connection between Apulia and Sahara continental margins in the Southern Apennines and in Sicily. Mem. Soc. Geol. It. 13, 317–323.

Shipton, Z.K., Cowie, P.A., 2001. Damage zone and slip-surface evolution over μm to km scales in high-porosity Navajo sandstone, Utah. Journal of Structural Geology 23, 1825–1844.

Sneider, R.M., Sneider, J.S., Bolger, G.W., Neasham, J.W., 1997. Comparison of seal capacity determinations—Core versus cuttings. Geological Society of America Memoir 67, 1–12.

Tondi, E., Piccardi, L., Cacon, S., Kontny, B., Cello, G., 2005. Structural and time constraints for dextral shear along the seismogenic Mattinata Fault (Gargano, southern Italy). Journal of Geodynamics 40, 134–152.

Tondi, E., Antonellini, M., Aydin, A., Marchegiani, L., Cello, G., 2006a. Interaction of deformation bands and stylolites in fault development in carbonate grainstones of the Majella Mountain, Italy. Journal of Structural Geology 28, 376–391.

Tondi, E., Zampieri, D., Alessandroni, M., Giunta, G., Renda, P., Unti, M., Giorgianni, A., Cello, G., 2006b. Active faults and inferred seismic sources in the San Vito lo Capo peninsula, north-western Sicily, Italy. Geological Society, London, Special Publications, vol. 262, pp. 365–377.

Vajdova, V., Baud, P., Wong, T.F., 2004. Compaction, dilatancy, and failure in porous carbonate rocks. Journal of Geophysical Research-Solid Earth 109(B5), Art. No. B05204.

Willemse, E.J.M., Peacock, D.C.P., Aydin, A., 1997. Nucleation and growth of strike-slip faults in limestones from Somerset, U.K. Journal of Structural Geology 19, 1461–1477.